Reactive Nitrogen in Asian Continental Outflow Over the Western Pacific: Results from the NASA TRACE-P Airborne Mission

R. Talbot[1*], J. Dibb[1], E. Scheuer[1], G. Seid[1], R. Russo[1], S. Sandholm[2], D. Tan[2], H. Singh[3], D. Blake[4], N. Blake[4], E. Atlas[5], G. Sachse[6], and M. Avery[6]

[1]University of New Hampshire, Durham, NH 03820
[2]Georgia Institute of Technology, Atlanta, Georgia 30332
[3]NASA Ames Research Center, Moffett Field, CA 94035
[4]University of California – Irvine, Irvine, CA 92716
[5]National Center for Atmospheric Research, Boulder, CO 80305
[6]NASA Langley Research Center, Hampton, VA 23665

*Institute for the Study of Earth, Oceans, and Space
Climate Change Research Center
39 College Road
University of New Hampshire
Durham, NH 03824
Phone: (603)862-1546
Fax: (603)862-2124
E-mail: robert.talbot@unh.edu

Submitted to: *Journal of Geophysical Research – Atmospheres*
Special Section on NASA TRACE-P

October 2002

Abstract. The NASA airborne mission TRAnsport and Chemical Evolution over the Pacific (TRACE-P) was conducted in February-March 2001. We present here results for reactive nitrogen species obtained aboard the DC-8 aircraft for flights conducted in the western Pacific west of 150°E longitude. This region is heavily influenced by continental outflow of Asian emissions at this time of the year. The data show close correspondence in the large-scale distribution of mixing ratios of total reactive nitrogen (NO_y = NO + NO_2 + HNO_3 + PAN + C_1-C_5 alkyl nitrates) and CO, a general tracer of combustion emissions. There was also a very general correlation between NO_y and O_3. Correlations of NO_y with CO and O_3 were better defined in the boundary layer with significant degradation of the relationships as altitude increased. Typically, NO_y was enhanced over background levels of ~300 pptv by 20-to-30-fold. The ratio C_2H_2/CO was used as an indicator of air parcel processing, and values of 1-4 were present at altitudes up to 10 km and as far eastward as 150ºE. Ratio values of this magnitude and their spatial distribution imply significant vertical mixing of air parcels over the Asian continent followed by rapid advective transport across the Pacific. Five Asian regions were identified as principal areal sources using an analysis of air parcel isentropic backward trajectories. Analysis of the chemistry of air parcels originating from these groupings showed that HNO_3 and PAN dominated NO_y in all regions, with HNO_3 comprising as much as 80% in the coastal category. NO_y and the unique combustion tracer C_2H_2 were very tightly correlated in the SE Asia group, but were only moderately related in the other groupings. Urban/industrial and biomass burning influences on the continental outflow composition were investigated using C_2Cl_4 and CH_3Cl respectively. Correlations of NO_y with C_2Cl_4 were not well defined in any of the source regions and they were only slightly better with CH_3Cl. Air parcels over the western Pacific appear to contain a complex mixture of emission sources that are not easily resolvable. This point was

reinforced by analysis of the composition of the Shanghai mega-city plume. It contained an intricate mixture of pollution emissions and exhibited the highest mixing ratios of NO_y species and other compounds that were observed during the TRACE-P campaign. Mixing ratios of C_2H_2 peaked at over 10,000 pptv and those of NO_y 12,000 pptv, with HNO_3 comprising 8,000 pptv of NO_y. C_1-C_5 alkyl nitrates totaled 100-200 pptv, being dominated by 2-$BuONO_2$ and i-$PrONO_2$. Comparison of tropospheric chemistry between the earlier PEM-West B mission and the recent TRACE-P data showed remarkable similarities and differences. These were most evident in the boundary layer where significant increases in the mixing ratios of NO_y species have occurred. However, the NO_y loading in the middle and upper troposphere seems to have been affected minimally by increasing emissions on the Asian continent over the last seven years.

1. Introduction

The TRAnsport and Chemical Evolution over the Pacific (TRACE-P) airborne mission was conducted by the National Aeronautics and Space Administration to better understand how outflow of anthropogenic emissions and crustal dust from the Asian continent affects the composition of the global atmosphere. The TRACE-P flights were designed to determine the pathways and chemical evolution of trace gases and aerosols transported to and across the north Pacific troposphere. TRACE-P built upon the results and experience from previous NASA missions conducted in this region in 1991 and 1994, the Pacific Exploratory Missions – West A and B respectively [*Hoell et al*., 1996; 1997].

PEM-West A was conducted in the September – October time frame and demonstrated the complex nature of emissions over the western Pacific. For example, in the lower troposphere continental outflow was enhanced in numerous combustion and industrial tracers but at higher altitudes the ratio C_2H_2/CO was <1.5 indicating much older inputs, possibly from European origin [*Talbot et al*., 1996]. In the upper troposphere air parcels were enhanced in CH_4 but depleted in CO_2 and COS, indicating potential biogenic emissions of CH_4 and vegetative uptake of CO_2 and COS.

A much more comprehensive sampling and analysis of Asian outflow was conducted during PEM-West B which revealed important subtle details. Backward 5-day isentropic trajectories and atmospheric chemistry together indicated that there was extensive rapid outflow from Asian continental areas below 5 km altitude [*Talbot et al*., 1997]. Aged marine air was rarely encountered over the western Pacific due to the strong late winter/springtime continental outflow, and then it was only sampled at latitudes <20^o N. The outflow at low altitude had significant enhancements of industrial tracers such as C_2Cl_4, CH_3CCl_3, and C_6H_6 intermixed with

the combustion products C_2H_2, C_2H_6, CO, and NO. In the middle-to-upper troposphere Middle Eastern and European source regions were implicated as possible contributors to the outflow. The importance of vertical convective transport was apparent, with subsequent removal of water-soluble species like HNO_3, SO_2, and H_2O_2. The long-range transport of PAN in the mid-troposphere with subsequent downward mixing and conversion to NO_x was postulated to be an important source of reactive nitrogen to the remote Pacific boundary layer [*Dibb et al*., 1997].

The rapid industrialization on the Asian continent is of compelling interest to atmospheric chemistry and climate change. Energy use in eastern Asia has increased by 5% yr^{-1} over the past decade and is expected to continue at this rate for several more decades [*U.S. Department of Energy*, 1997]. Combustion of fossil fuels is the main source of energy, with emissions of NO_x predicted to increase nearly 5-fold by 2020 [*van Aardenne*, 1999].

The suite of NASA western Pacific missions has observed the time-dependent impact on the northern hemispheric tropospheric chemistry of a major industrial revolution on the Asian continent. Long-term observations from ground sites provide a continuous framework, but aircraft and satellite observations significantly augment our understanding of dynamical and chemical processes affecting atmospheric composition over a large remote geographic region like the Pacific basin. TRACE-P is the most recent NASA mission in the Pacific Rim region and it provided a detailed chemical characterization of Asian continental outflow and emissions. In this paper we focus specifically on the suite of reactive nitrogen species, which are critical in determining the overall compositional mixture of chemical species in continental outflow over the north Pacific. This outflow is expected to begin to influence atmospheric chemistry over North America within the current decadal time frame [*Bernsten and Karlsdottir*, 1999; *Jacob et al*., 1999].

2. Airborne Mission

The airborne component discussed in this paper was conducted aboard the NASA Dryden DC-8 research aircraft. Transit and intensive science missions comprised 20 flights, with each one averaging ~ 8 hours in duration and covering an altitude range of 0.3 - 12.5 km. The flights over the western Pacific, from which the data for this paper are drawn, were centered in the region west of 150°E longitude. The base of operations for these flights was from Hong Kong (six flights) and Yokota, Japan (eight missions).

The overall scientific rationale and description of the individual aircraft missions is described in the TRACE-P overview paper [*Jacob et al*., this issue]. The features of the large-scale meteorological regime and associated air parcel backward trajectory analyses for the February – March 2001 time frame are presented by *Fuelberg et al*. [this issue]. A general description of the chemical composition of the Asian continental outflow is in a companion paper [*Russo et al*., this issue].

We present here a broad description of the outflow chemistry focused on the reactive nitrogen family and refer to the overview paper [*Jacob et al*., this issure] and companion papers for descriptions of the various measurements. Additionally, more specific information is included below for measurement details of the reactive nitrogen species. Since total reactive nitrogen (NO_y) was not measured on the DC-8, we use the sum of NO, NO_2, PAN, HNO_3, and C_1-C_5 alkyl nitrates to represent NO_y. Aerosol nitrate was not included in NO_y since its contribution to NO_y rarely exceeded 5%, and because its measurement time base (~10 minutes) was substantially longer than that for gas phase species.

NO and NO_2 were measured by the Georgia Institute of Technology using photofragmentation two-photon laser-induced fluorescence (TP-LIF) [*Sandholm et al*., 1990].

The method spectroscopically detects NO, with UV laser photolysis of NO_2 and subsequent detection of NO. The optical detection scheme involves sequentially exciting rotationally resolved transitions in the $X^2II - A^2\sum$ and the $A^2\sum - D^2\sum$ bands of NO using laser wavelengths centered at 226 nm and 1.1 μm respectively. The resulting blue shift in fluorescence is monitored near 190 nm. Calibration utilized a NIST certified NO standard (±1-2%). The precision and accuracy of the measurements are estimated to be on the order of 20-30%. The sampling inlet was comprised of a 10 cm ID glass coated (vapor deposited) intake flowing by ram force at ~$6x10^3$ cm s^{-1}, giving a residence time of 40 ms. The details of the entire system are described in *Bradshaw et al*., [1999].

PAN was measured by NASA Ames Research Center using cryogenic pre-concentration of ambient air and analysis of it using gas chromatography with electron capture detection. PAN was measured every 5 minutes aboard the DC-8 by an electron-capture gas-chromatographic technique [*Singh et al*., 2001]. Typically, 160 ml of ambient air was pre-concentrated at -140°C over a 2-min period. PAN calibrations were performed by using a 2-ml diffusion tube filled with pure liquid PAN in a *n*-tridecane matrix. A dynamic dilution system was used to generate low-pptv mixing ratios of PAN. The technique has a measurement sensitivity of better than 1 pptv PAN. Instrument precision and accuracy are estimated to be ±10% and ±25% respectively. Inter-comparison studies performed during Trace-P further confirmed that the reliability of the PAN measurements was within these specifications [*Eisele et al*., this issue].

Nitric acid was measured by the University of New Hampshire using the mist chamber/ion chromatography technique [*Talbot et al.*, 2000]. Sampling was conducted using a high-flow manifold (3,000 liters per minute) that was glass coated (vapor deposited) and heated to 50ºC. The manifold was 8 cm ID and had a diffuser configuration over the entrance to boost

the flow/pressure and facilitate sampling at the high velocities (Mach 0.88) of the DC-8. The inlet design was nearly identical to that used for NO/NO_2 [*Bradshaw et al*., 1999] and OH/HO_2 [*Brune et al*., 1998]. The inlet was equipped with the capability to conduct standard additions of HNO_3 into the manifold and quantify its passing efficiency frequently during flight. A permeation source was used for HNO_3 from which the output was tracked using Nylon filters and a NO_x chemiluminescence instrument equipped with a molybdenum NO_y converter heated to 350ºC. The output of the permeation source was about 200 ppbv of HNO_3 that could be readily diluted to pptv levels and quantified in our manifold. Thus, standard additions were conducted at approximately twice ambient HNO_3 mixing ratios. The precision and accuracy of the HNO_3 measurements are both in the range of 10-20% depending on the ambient mixing ratio. The time resolution of the ambient measurements was two minutes. Inter-comparisons with a chemical ionization mass spectrometer instrument aboard the NASA P-3 aircraft during TRACE-P showed good agreement (± 20%) under most atmospheric conditions [*Eisele et al*., this issue].

Alkyl nitrate species were measured by the University of California – Irvine and the National Center for Atmospheric Research (NCAR) after collection of ambient air samples in 2-liter electropolished stainless steel canisters. A two-stage metal bellows pump was used to pressurize the canisters to 3.8 hPa. Samples were obtained every 3-7 minutes during horizontal flight legs with a collection interval of 8 s at 150 m to 90 s at 12 km. The following alkyl nitrates were measured in each sample: methyl nitrate (CH_3ONO_2), ethyl nitrate ($C_2H_5ONO_2$), n-propyl nitrate (n-$C_3H_7ONO_2$), i-propyl nitrate (i-$C_3H_7ONO_2$), 2-butyl nitrate (2-$C_4H_9ONO_2$), 2-pentyl nitrate (2-$C_5H_{11}NO_3$), and 3-pentyl nitrate (3-$C_5H_{11}NO_3$). The analytical procedures are detailed in *Colman et al*. [2001]. The C_1-C_5 alkyl nitrates were separated using three of the five column-detector combinations in the UC-Irvine laboratory. The limit of detection for alkyl

nitrates was typically 0.02 pptv with a precision of ±5% at mixing ratio >5 pptv and ±10% below 5 pptv. Calibration for alkyl nitrates used regular analysis of whole air standards which were inter-calibrated with synthetic air standards prepared at NCAR.

3. General Trends Over the Western Pacific

To present the overall distribution of reactive nitrogen over the western Pacific, the entire one minute data set for flights 6 – 17 was utilized. For species with a time response greater than 1 minute, duplicated values generated by the merging process were removed from the database. Data collected above 7 km altitude was filtered additionally to remove stratospheric air influences using O_3 (>120 ppbv), CO (<70 ppbv), and dew point temperature (< -50°C) values indicative of stratospheric influence. However, the air parcels in this region often had both combustion and stratospheric influences superimposed, so it was impossible to completely remove the stratospheric component.

The latitudinal distributions of NO_y and CO are presented in Figure 1, and they illustrate the widespread influence of combustion emissions on atmospheric chemistry over the western Pacific. The close correspondence in the distribution of mixing ratios of CO and NO_y suggests a direct source relationship between combustion and reactive nitrogen species. Indeed, at all altitudes in the latitudinal band of 20-40 °N well-defined plumes contained NO_y in excess of 1000 pptv.

The relationship between NO_y and CO is shown in Figure 2. The correspondence in NO_y and CO was most apparent in the boundary layer and was not well defined at altitudes above it. Presumably this reflects sampling of less processed air parcels down low and the closeness of major emission sources on the Asian continent. Even in the boundary layer the relationship between NO_y and CO was strongly driven by sampling of heavily polluted plumes advected over

the Pacific Rim region from concentrated urban centers such as Shanghai. At higher altitudes the air parcels had undergone more processing and they are also likely impacted by both Asian and other more distant sources. For example, a European influence was hypothesized for altitudes >7 km over the western Pacific during the PEM-West B time frame [*Talbot et al*., 1997a].

Photochemical processing of air parcels that have NO_x-rich hydrocarbon mixtures leads to production of a suite of reactive nitrogen compounds and O_3. Thus, the correspondence between NO_y and O_3 is of interest. In general, the correlations between NO_y and O_3 were poorly defined in the Asian outflow over the western Pacific (Figure 2). As in the case of CO, the tightest relationship was found in the boundary layer, where it was again determined largely by the most heavily polluted plumes. In the mid-troposphere the values were centered on an O_3 mixing ratio of 60 ppbv, with NO_y being as high as 2,500 pptv. Observations very similar to these reported here were obtained during PEM-West B, except that it was centered on O_3 mixing ratios in the 40-50 ppbv range [*Koike et al*., 1997]. Above 7 km altitude there was a weak linear trend in NO_y and O_3 that may be related to the strong linear correspondence between these species in stratospheric air [*e.g*., *Talbot et al*., 1997b]. As stated earlier, air parcels in this region were influenced coincidently by combustion and stratospheric sources which could not be separated adequately. Alternatively, the positive correlation could have been the result of biomass burning emissions occurring in southeastern Asia. This point is addressed further in this paper when we examine specific characteristics of various Asian source regions based on analysis of air parcel backward trajectories.

Anthropogenically influenced air parcels a few hundred kilometers from point sources typically exhibit values of NO_y/O_3 of 0.1-0.2 in the U.S. [*Trainer et al*., 1991]. Northern hemispheric background air, that is, well processed aged parcels that have not been influenced by

emissions recently, have NO_y/O_3 ratios in the range 0.005-0.015 [*Talbot et al.*, 1994]. The smallest values tend to occur at altitudes below 3 km, presumably due to removal of HNO_3 by precipitation scavenging and dry deposition. Using median values for the three altitude bins illustrated in Figure 2, NO_y/O_3 ratios were estimated to be on the order of 0.03 in the boundary layer and 0.004 in the mid-to-upper troposphere over the western Pacific. In general, the large-scale spatial distribution of the ratio is not well known, but its variability should be closely related to the nitrogen content of local emissions and associated photochemical tendency of the affected air parcels. The values that we observed over the western Pacific appear to be somewhat lower than those measured over North America. However, such comparisons are tenuous due to seasonal differences between the North American and Pacific data sets and variations in regional meteorology with respect to precipitation scavenging of soluble NO_y.

The latitudinal pattern of individual reactive nitrogen species over the western Pacific is presented in Figure 3. For the most part, mixing ratios of NO_x were <100 pptv, suggesting that the sampled air parcels were aged at least 1-2 days which allowed for transformations of it to HNO_3, PAN, and other NO_y species. The largest enhancements in all species occurred at 30 °N when the DC-8 sampled the Shanghai mega-city urban plume during a boundary layer leg over the Yellow Sea. This plume contained mixing ratios of NO_x, HNO_3, PAN, and alkyl nitrates of up to 3,000, 8,000, 4,300, and 225 pptv respectively. In a later section of this paper we discuss the chemical composition of this plume in detail.

The vertical distribution of reactive nitrogen species provides insight to the nature of their sources, and in particular the association of origin either on the Asian continent or from long-range transport into the western Pacific region. These distributions are summarized in Figure 4, where the alkyl nitrate species are represented as the sum of the individual species (*i.e.*, sum

Alkyl-ONO_2). Shown also is aerosol nitrate based on Teflon filter measurements with approximately 10 minute time resolution as described in *Dibb et al*. [this issue].

All the gas phase reactive nitrogen species showed significant deviations and enhancements well above their background values, defined as the median of the lowest 15% of the observed mixing ratios at a given altitude. The background mixing ratios exhibited little altitude dependence, and representative values were as follows: NO_x (25 pptv), HNO_3 (125 pptv), PAN (100 pptv), alkyl nitrates (7 pptv), aerosol nitrate (25 pptv), and NO_y (300 pptv). The enhancements occurred at all altitudes up to the 12 km ceiling of the DC-8 aircraft. It was not uncommon for the enhanced mixing ratios to be 10-to-20-fold larger than their corresponding background value. Particularly noteworthy were the alkyl nitrate species which exhibited combined increases of up to 50 pptv at altitudes up to 8 km. The alkyl nitrate distribution was dominated by 2-butyl nitrate which comprised on average 30% of the sum depicted in Figure 4.

The largest mixing ratios of aerosol nitrate were observed in the Asian coastal marine boundary layer. On some occasions ppbv values of aerosol nitrate were measured that far exceeded attendant mixing ratios of HNO_3. Undoubtedly, the high levels of nitrate reflected uptake of HNO_3 by sea salt aerosols, as evidenced by coincidently large mixing ratios of sodium and chloride [*Dibb et al.*, this issue].

An important consideration for interpretation of the TRACE-P observations is the relative processing of air parcels over various spatial and temporal scales. Here we use the ratio C_2H_2/CO as a scaling factor in this regard. The distribution of the values of this ratio over the western Pacific provides key insight into transport and mixing processes on various time scales. The vertical altitudinal ensemble of values in C_2H_2/CO is presented in Figure 5 along with the longitudinal variation. The distributions are striking; ratio values in the mid-to-upper

troposphere mimic the boundary layer and also indicate transport of continent emissions across the Pacific. Further, the data suggest that frontal uplifting and vertical transport is rapid and operating continuously over the Asian continent in combination with extensive westerly transport of pollutants at all altitudes. This result explains the blurred correlations between NO_y and CO or O_3. The continuous intermixing of air parcels of various ages and processing would lead directly to very complex distributions and relationships of NO_y, CO, and O_3 over the western Pacific, which is exactly what we observed.

An important transport pattern over Asia during winter is bifurcation of westerly flow when it passes over the Tibetan Plateau. Here the northern branch forms many blocked anticyclones while the southern one forms many troughs or cut-off lows, such as the Bangladesh trough and other troughs in southern China. The two branches merge at the eastern edge of the Plateau, resulting in strong winds over the southern Sea of Japan, where the maximum wind speed can reach over 70 m s^{-1} at 500 mb [*Zhang*, 1992]. Such a dynamic system is conducive to the occurrence of unstable weather systems in southern China in winter. The associated dynamical processes help explain why the TRACE-P data show pollutants mixed to high altitudes and transported eastward rapidly to 150ºE.

4. Relationships Based on Source Region Apportionments

To examine the detailed relationships of NO_y species with source tracer species and their spatial variability, air parcel backward trajectories were used to establish the principal source region locations on the Asian continent. Isentropic backward trajectories were provided by the Florida State University for TRACE-P, and a description of the method is provided in *Fuelberg et al*. [this issue]. For consistency with other TRACE-P analyses, we adopted the source region designations in this paper determined by *Russo et al*. [this issue] and *Jordan et al*. [this issue].

Five regions were identified in their analyses as depicted in Figure 6. These were classified as follows: (1) north-northwest (NNW), (2) west-southwest (WSW), (3) southeast Asia (SE Asia), (4) coastal and, (5) central. The major urban/industrial centers in China are located within the coastal and central source regions.

Since we have introduced the general latitudinal and vertical distributions of reactive nitrogen species for the western Pacific region, more specific source region relationships are presented here. We begin with the altitudinal budget of NO_y species in the various source regions (Figure 7). In the southeast and coastal groups, HNO_3 dominated NO_y in the boundary layer and mid-troposphere. This was especially true for the coastal group where HNO_3 comprised nearly 80% of NO_y. There were nearly equal contributions from HNO_3 and PAN in the other three source regions, with PAN favored in the NNW and WSW groups at all altitudes. These distributions are consistent with expectations of less PAN in warmer locations due to its thermal instability and more PAN at higher altitudes where it is more stable. The predominance of HNO_3 and PAN in the NO_y budget indicates that the majority of sampled air parcels were aged several days with significant photochemical processing over that time interval. It is not clear why NO_x comprised 20-25% of NO_y in the mid-to-upper troposphere in the WSW group. This finding was quite different than in the other four groups where its contribution was <10%. Possibilities include recent inputs from sources such as biomass burning and stratospheric inputs, or decreased photochemical activity (*i.e.*, less efficient conversion to other NO_y species).

Together these data indicate that significant outflow of reactive nitrogen occurs at all altitudes from the Asian continent with much of it residing in reservoir species like PAN. Due to its long lifetime in the middle and upper troposphere, it can subsequently carry reactive nitrogen over long distances and be a source of NO_x to various areas of the northern hemisphere

troposphere. During PEM-West B strong outflow in the mid-troposphere contained high levels of PAN, and *Dibb et al*. [1997] hypothesized that it was a significant source of NO_x and subsequently aerosol nitrate to the remote marine boundary layer over the central Pacific.

To assess the regional combustion influence on the NO_y distribution over the western Pacific, correlations between C_2H_2 and NO_y were examined for the five primary Asian source areas defined in Figure 6. These relationships are illustrated in Figure 8. To the best of our understanding, the only source of C_2H_2 to the atmosphere is combustion [*Singh and Zimmerman*, 1992]. NO_y and C_2H_2 were highly correlated in the SE Asia region, and to a lesser extent in the central and coastal groups. The central group was the most potent combustion source of NO_y based on the slopes given in Figure 8. There was little or no correlation between these species in the NNW and WSW regions. These two regions are the farthest from the western Pacific, and as such have likely undergone more atmospheric processing than the other groups. The source relationships are consequently more blurred in these datasets. As presented previously, the WSW group also showed the largest mixing ratios of NO_x above 7 km of all five source regions. The apparent low correlation with combustion suggests that the NO_x may be related to stratospheric inputs or be from re-cycled reactive nitrogen in the upper troposphere. However, why these NO_x sources would only affect this one region is unclear.

To check for stratospheric inputs, correlations were examined between NO_x and H_2O vapor, dew point, O_3, and HNO_3 in upper troposphere for the WSW group. The relationships between NO_x and O_3 or HNO_3 showed significant scatter on a linear plot. However, there was a trend of higher mixing ratios of NO_x occurring coincidently with low mixing ratios of H_2O vapor and dew point temperature (Figure 9). These trends lean toward a stratospheric source for the enhanced upper tropospheric NO_x in the WSW group.

C_2Cl_4 is released exclusively by urban/industrial processes [*Blake et al*.., 1996], and as such is a good tracer of air parcels influenced by metropolitan areas. In the central and coastal groups there were very general relationships between NO_y and C_2Cl_4, but in the other groups it was poorly defined (Figure 10). We examined correlations between individual NO_y component species and they too showed no clear correspondence with C_2Cl_4. However, it appears that the use or release of C_2Cl_4 has decreased since the PEM-West B mission. *Russo et al*. [this issue] found that median values of C_2Cl_4 were about 2-fold less than those observed in the PEM-West B study. This reduced urban/industrial signal probably contributed to the weak correlations between NO_y and C_2Cl_4 during TRACE-P. As indicated by the central group, concentrated urban sources of C_2Cl_4 still do exist on the Asian continent. Mixing ratios of C_2Cl_4 peaked near 125 pptv when the Shanghai urban plume was sampled over the Yellow Sea.

Biomass burning on the Asian continent is expected to be a large source of NO_y [*Streets et al*., this issue]. These emissions originate from fossil fuel combustion, bio-fuels for space heating and cooking, and agricultural practices. Good tracers of biomass burning emissions include soot carbon, fine aerosol potassium and ammonium, and CH_3Cl [*Crutzen et al*., 1979; *Crutzen and Andrea,* 1990]. Here we have chosen to use CH_3Cl due to its availability on a one-minute time basis. The NO_y correlations with CH_3Cl over the western Pacific are depicted in Figure 11. The tightest correspondence was observed for the central source region, but it is entirely driven by sampling of the Shanghai plume. There were weak correlations in the SE Asia and coastal groups, and none in the NNW and WSW areas. This is a bit unexpected, especially for the SE Asian region where extensive biomass burning was indicated there by satellite surveying during the TRACE-P time period (http://www.people.fas.harvard.edu/~heald/fires.html).

Overall, it appears that air parcels advected from over the Asian continent to the western Pacific rarely contained a unique source signal. Both C_2Cl_4 and CH_3Cl, which are fairly specific tracers of urban and biomass burning emissions respectively, provided minimal insight to the relative importance of these sources. For urban/industrial tracers we expanded our efforts to include CH_3CCl, Halon-1211, and CH_3Br (enhanced greatly in Japanese urban areas). None of these improved the source recognition issues. Most distributions were centered commonly around the median mixing ratio of the tracer species employed in the analysis. This result implies that we must rely more than ever on meso-scale modeling results and associated emission inventories to facilitate our understanding of continental scale atmospheric chemistry and inter-continental transport.

5. Characterization of the Shanghai Plume

The Shanghai urban plume was sampled during flight 13 at 0.34 km altitude over the Yellow Sea. This plume contained the largest mixing ratios of most species, with O_3 being one exception, observed during the TRACE-P mission. The plume was a combination of various age air parcels, with the freshest components exhibiting a C_2H_2/CO ratio of 9.3, and the rest in the 4-6 range (Figure 5). These values suggest a well defined plume with emissions of at most a day old.

The large mixing ratios of highly reactive species such as C_2H_4 are evidence of the very recent emissions associated with the Shanghai plume (Figure 13). The combustion nature of the plume was captured by the very high levels (~10,000 pptv) of C_2H_2. The urban/industrial signature of the plume contained a large ensemble of enhanced volatile organic compounds, including C_2Cl_4 and CH_3Br (Figure 13). Mixing ratios of CH_3Cl reached 1600 pptv (3 times

background levels), indicating that a strong biomass burning component also influenced the chemical composition of the plume (not shown).

Since the Shanghai plume appears to represent a significant source of reactive nitrogen to marine boundary layer over the western Pacific, we examined its NO_y budget in detail. This included examination of the distribution of individual NO_y species, plus a breakdown of the seven alkyl nitrate compounds measured by the UCI-NCAR groups. These data show that i-propyl and 2-butyl nitrate were the most abundant alkyl nitrate species in this urban/industrial plume. Their peak mixing ratios were ~70 pptv, followed by the pentyl nitrates at 20-25 pptv. Methyl and ethyl nitrate were among the least abundant, opposite to their distribution over the tropical Pacific where they appear to be released from the surface ocean contributing to the 30-50 pptv levels typical of the remote marine boundary layer [*Talbot et al*., 2000; *Blake et al*., 2002]. Together the alkyl nitrate sum exceeded 200 pptv in the heart of the plume, a very significant amount but still less than 2% of total NO_y.

The distribution of individual NO_y species showed the following approximate contributions: NO_x (15%), HNO_3 (53%), PAN (30%), and alkyl-ONO_2 (2%). At one point in the marine boundary layer aerosol nitrate reached 13,500 pptv in the plume [*Dibb et al*., this issue]. Thus, it was equal to or greater than total gas phase NO_y. This finding suggests that the Shanghai plume contains very large mixing ratios of HNO_3 over the Asian continent, but that it is rapidly lost to sea salt aerosols over the ocean. Together the HNO_3 and aerosol nitrate must exceed 20,000 pptv over the Asian continent, with HNO_3 likely dominating the phase partitioning. Formation of PAN may be hindered by availability of precursors. However, a principal precursor such as acetone was present in the plume at up to 6,500 pptv levels (not shown). These data indicate that OH levels in the plume are probably controlled to a large extent

by reaction with NO_2 to form HNO_3. However, detailed measurements are required over the Asian continent to confirm such speculations concerning this mega-city urban/industrial plume.

6. Comparison of TRACE-P to PEM-West B Results

Due to rapid industrialization on the Asian continent, it is of great interest to examine changes in tropospheric chemistry over the western Pacific during the past decade. Since PEM-West B was conducted during the same monthly time frame in 1994 that TRACE-P covered in 2001, direct meaningful comparisons are possible. In addition, many of the species were measured by the same investigator groups during both missions, minimizing measurement biases.

Russo et al. [this issue] found few changes in the distributions and mixing ratios of a large suite of trace gases. One exception to this was O_3, which appears to have increased by 10-20 ppbv throughout the western Pacific. There was a very significant increase in the mixing ratios of water-soluble aerosol species during TRACE-P compared to PEM-West B [*Dibb et al*., this issue]. It is difficult to access how much of the 2-5 fold increases were due to emissions compared to other confounding factors such as variations in the degree of precipitation scavenging.

For the comparisons we used summary statistics for the PEM-West B period reported by *Talbot et al*. [1997a]. The PEM-West B data were broken into two groups, continental north and south, divided by a geographic separation at 20° N. We thus compared the continental north group with the TRACE-P coastal, central, and NNW groups, and the continental south region with the SE Asia group. The WSW group was not used in these comparisons since it overlaps significantly with both PEM-West B source regions. Furthermore, NO_2 and the alkyl nitrate species were not measured during PEM-West B. The values of NO_y for that mission were

measured by Georgia Tech using TP-LIF detection of NO after reduction of NO_y species using a gold converter system [*Bradshaw et al.*, 1998].

Tables 1 and 2 contain a summary of NO_y species comparisons for the two western Pacific missions. In the boundary layer for the northern groupings median mixing ratios of HNO_3 and PAN were 2-5 times higher during TRACE-P compared to PEM-West B. An exception was for PAN in the coastal group. Although most of the differences in mean values are statistically significant (t-test, P = 0.05), the maximum values are relatively similar. The comparisons for NO_y are not significantly different except for the central group at 0-2 km altitude where they were much greater than the PEM-West B results (P = 0.05). Comparisons for the middle and upper troposphere revealed a remarkable similarity over the seven year period between the missions. The only significant difference was for HNO_3 in the coastal group where the mean values for TRACE-P were a factor of 2 higher than in PEM-West B (P = 0.05).

Comparisons of the continental south group with the TRACE-P SE Asia group showed that differences existed but they did not vary in a systematic manner. In the boundary layer median mixing ratios of HNO_3 and NO_y were 8- and 6-fold lower respectively during TRACE-P. This may be due to the fact that during PEM-West B relatively few data were obtained in the continental south region [*Talbot et al.*, 1997b]. We clearly did not get a good statistically sampling of air parcels in 1994 so the results are unlikely to be representative of that region. It may be fortuitous for the previous reason that the middle and upper tropospheric data are similar for both missions. Nevertheless, it appears that in general that the NO_y loading above the boundary layer has been affected minimally by increasing emissions on the Asian continent over the last seven years. The data show that the biggest changes and influences were in the boundary layer.

7. Summary

We presented the general distributions of NO_y and individual NO_y species over the western Pacific during the TRACE-P study period of February-March 2001. In general, NO_y was dominated by HNO_3 and PAN, while NO_x mixing ratios were commonly <100 pptv except in plumes where they exceeded 1000 pptv on a few occasions. There was a significant combustion influence over the western Pacific, as evidenced by the distributions of CO and C_2H_2. Correlations of NO_y with an urban tracer such as C_2Cl_4 and CH_3Cl for biomass burning were not well defined in most cases.

The distribution of the ratio C_2H_2/CO was striking, showing values in the mid-to-upper troposphere that mimicked the boundary layer and ones that support a scenario of rapid advective transport of continent emissions across the Pacific to at least 150°E. These findings suggest that extensive frontal uplifting and vertical transport is operating continuously over the Asian continent combined with extensive westerly transport of pollutants at all altitudes. This result helps explain the blurred correlations observed between NO_y and CO or O_3. Such continuous intermixing of air parcels of various ages and processing would lead directly to the very complex distributions and relationships that we observed for NO_y, CO, and O_3.

On one occasion the Shanghai mega-city plume was characterized during a flight over the Yellow Sea. The plume was intercepted at 0.34 km altitude and exhibited peak mixing ratios of more than10,000 pptv C_2H_2, 3,000 pptv C_2H_4, 12,000 NO_y, 8,000 pptv HNO_3, and 30 pptv CH_3Br. C_1-C_5 alkyl nitrates totaled 100-200 pptv, being dominated by 2-$BuONO_2$ and i-$PrONO_2$. Our results suggest that the Shanghai plume represents a significant source of reactive nitrogen to the marine boundary layer over the western Pacific.

Comparison of results between the earlier PEM-West B mission and the recent TRACE-P campaign show remarkable similarities in tropospheric chemistry. This was most evident in the middle and upper troposphere where NO_y loadings appear to have been affected minimally by increasing emissions on the Asian continent over the last seven years. However, significant increases in the mixing ratios of NO_y species were readily apparent in the boundary layer.

Acknowledgments. We appreciate the support provided by the DC-8 flight and ground crews at the NASA Dryden Flight Research Center. This research was supported by the NASA Global Tropospheric Chemistry program in the Office of Earth Science.

References:

Bernsten, T. K., and S. Karlsdottir, Influence of Asian emissions on the composition of air reaching the North Western United States, *Geophys. Res. Lett.*, *26*, 2171-2174, 1999.

Blake, D. R., T. –Y. Chen, T. W. Smith, Jr.,, C. J. –L Wang, O. W. Wingenter, F. S. Rowland, and E. W. Mayer, Three dimensional distribution of NMHCs and halocarbons over the northwestern Pacific during the 1991 Pacific Exploratory Mission (PEM-West A), *J. Geophys. Res.*, *101*, 1763-1778, 1996.

Blake, Nicola J., Donald R. Blake, Aaron L. Swanson, Elliot Atlas, Frank Flocke, and F. Sherwood Rowland, Latitudinal, vertical, and seasonal variations in C_1-C_4 alkyl nitrates in the troposphere over the Pacific Ocean during PEM-Tropics A and B: Oceanic and continental sources, *J. Geophys, Res*., in press, 2002.

Bradshaw, J., S. Sandholm, and R. Talbot, An update on reactive odd-nitrogen measurements made during recent NASA Global Tropospheric Experiment programs, *J. Geophys. Res.*, *103*, 19,129-19,148, 1998.

Bradshaw, J., D. Davis, J. Crawford, G. Chen, R. Shetter, M. Muller, G. Gregory, G. Sachse, D. Blake, B Heikes, H. Singh J. Mastromarino, and S. Sandholm, Photofragmentation two-photon laser-induced detection of NO_2 and NO: Comparison of measurements with model results based on airborne observations during PEM-Tropics A, *Geophys. Res., Lett., 26*, 471-474, 1999.

Brune, W. H., I. C. Faloona, D. Tan, A. J. Weinheimer, T. Campos, B. A. Ridley, S. A. Vay, J. E. Collins, G. W. Sachse, L. Jaegle, and D.J. Jacob, Airborne in-situ OH and HO_2 observations in the cloud-free troposphere and lower stratosphere during SUCCESS, *Geophys. Res. Lett*., *25*, 1701-1704, 1998.

Crutzen, P. J;., L. E. Heidt, J. P. Krasnec, W. H. Pollock, and W. Seiler, Biomass burning as a source of atmospheric gases CO, H_2, N_2O, NO, CH_3Cl, and COS, *Nature*, *282*, 253-256, 1979.

Crutzen, P. J., and M. O. Andreae, Biomass burning in the tropics: Impact on atmospheric chemistry and biogeochemical cycles, *Sceince*, *250*, 1669-1678, 1990.

Colman, J. J., A. L. Swanson, S. Meinarde, D. R. Blake, Description of the analysis of a wide range of volatile organic compounds in whole air samples collected during PEM-Tropics A and B, *Anal. Chem*. *73*, 3723-3731, 2001.

Dibb, J. E., R. W. Talbot, B. L. Lefer, and E. Scheuer, Distributions of beryllium-7 and lead-210 over the western Pacific: PEM-West B, February-March 1994, *J. Geophys. Res.*, *102*, 28,287-28,302, 1997.

Dibb, J. E., R. W. Talbot, E. Scheuer, and G. Seid, Aerosol chemical composition in Asian continental outflow during TRACE-P: Comparison to PEM-West B, *J. Geophys. Res*., this issue.

Eisele F., et al., Inter-comparison of selected atmospheric species on the NASA DC-8 and P-3 during TRACE-P, *J. Geophys. Res*., this issue.

Fuelberg, H., C. M. Kiley, J. R. Hannan, D. J. Westberg, M. A. Avery, and R. E. Newell, Atmospheric transport during the TRAnsport and Chemical Evolution over the Pacific (TRACE-P) experiment, *J. Geophys. Res*., *this issue*.Jordan, C., et al., *J. Geophys. Res*., this issue.

Hoell, J. M., D. D. Davis, S. C. Liu, R. Newell, M. Shipman, H. Akimoto, R. J. McNeal, R. J. Bendura, and J. W. Drewery, Pacific Exploratory Mission – West A (PEM-West A): September-October 1991, *J. Geophys. Res*., *101*, 1641-1653, 1996.

Hoell, J. M., D. D. Davis, S. C. Liu, R. E. Newell, H. Akimoto, R. J. McNeal, and R. J. Bendura, The Pacific Exploratory Mission-West Phase B: February-March, 1994, *J. Geophys. Res*., *102*, 28,233-28,239, 1997.

Jacob, D. J., J. A. Logan, and P. P. Murti, Effect of rising Asian emissions on surface ozone in the United States, *Geophys. Res. Lett*., *26*, 2175-2178, 1999.

Jacob, D. J., et al., Overview of the Transport and Chemical Evolution over the Pacific (TRACE-P) mission, *J. Geophys. Res*., this issue.

Jordan, C.,

Koike, M., Y. Kondo, S. Kawakami, H. Nakajima, G. L Gregory, G. W. Sachse, H. B. Singh, E. V. Browell, J. T. Merrill, and R. E. Newell, Reactive nitrogen and its correlation with O_3 and CO over the Pacific in winter and early spring, *J. Geophys. Res*., 102, 28,385-28,404, 1997.

R. Russo, R. Talbot, J. Dibb, E. Scheuer, G. Seid, S. Sandholm, D. Tan, H. Singh, D. Blake, N. Blake, E. Atlas, C. Jordan, G. Sachse, M. Avery, S. Vay, J. Snow, B. Heikes, Chemical composition of Asian continental outflow over the western Pacific: Results from TRACE-P, *J. Geophys. Res*., this issue.

Sandholm, S., J.D. Bradshaw, K. S. Dorris, M. O. Rogers, and D. D. Davis, An airborne-compatible photofragmentation two-photon laser-induced fluorescence instrument for measuring background tropospheric NO, NO_x, and NO_2, *J. Geophys. Res*., *95*, 10,155-10,161, 1990.

Singh, H. B., and P. B. Zimmerman, Atmospheric distribution and sources of nonmethane hydrocarbons, in *Gaseous Pollutants: Characterization and Cycling*, John Wiley, New York, 1992.

Singh, H, Y. Chen, A Staudt, D. Jacob, D. Blake, B. Heikes, J. Snow, Evidence from the Pacific troposphere for large global sources of oxygenated organic compounds, *Nature, 410*, 1078-1081, 2001.

Streets, D.G., T.C. Bond, G.R. Carmichael, S. Fernandes, Q. Fu, D. He, Z. Klimont, S.M. Nelson, N.Y. Tsai, M.Q. Wang, J.-H. Woo, and K.F. Yarber, A year-2000 inventory of gaseous and primary aerosol emissions in Asia to support TRACE-P modeling and analysis, *J. Geophys. Res.*, this issue.

Talbot, R. W., et al., Summertime distribution and relations of reactive odd nitrogen species and NO_y in the troposphere over Canada, *J. Geophys. Res.*, *99*, 1863-1885, 1994.

Talbot, R. W., et al., Chemical characteristics of continental outflow from Asia to the troposphere over the western Pacific Ocean during September – October 1991: Results from PEM-West A, *J. Geophys. Res.*, *101*, 1713-1725, 1996.

Talbot, R. W., *et al*., Chemical characteristics of continental outflow from Asia to the troposphere over the western Pacific Ocean during February – March 1994: Results from PEM-West B, *J. Geophys. Res.*, *102*, 28,255-28,274, 1997a.

Talbot, R. W., J. E. Dibb, B. L. Lefer, E. Scheuer, J. D. Bradshaw, S. T. Sandholm, S. Smyth, D. R. Blake, N. J. Blake, G. W. Sachse, J. E. Collins, Jr., and G. L. Gregory, Large-scale distributions of tropospheric nitric, formic, and acetic acids over the western Pacific basin during wintertime, *J. Geophys. Res.*, *102*, 28,303-28,313, 1997b.

Talbot, R. W., J. E. Dibb, E. M. Scheuer, J. D. Bradshaw, S. T. Sandholm, H. B. Singh, D. R. Blake, N. J. Blake, E. Atlas, and F. Flocke, Tropospheric reactive odd nitrogen over the South Pacific in austral springtime, *J. Geophys. Res*., *105*, 6681-6694, 2000.

Trainer, M., et al., Observations and modeling of the reactive nitrogen photochemistry at a rural site, *J. Geophys. Res*., *96*, 3045-3063, 1991.

U.S. Department of Energy, International Energy Outlook (IEO), Energy Information Administration, Available from http://www.eia.doe.gov/oiaf/ieo97, 1997.

Van Aardenne, J. A., G. A. Carmichael, H. Levy II, D. Streets, and L. Hordijk, Anthropogenic NO_x emissions in Asia in the period 1990-2020, *Atmos. Environ*., *33*, 633-646, 1999.

Zhang, Y., *Synoptic meteorology and climate*, Meteorology Press, Beijing, China, pp. 600-601, 1992.

Table 1. TRACE-P Nitrogen Budget Summary Statistics.

Source Region		NO_X	PAN	HNO_3	Sum Alkyl-ONO_2	NO_y*
NNW						
0-2 km	mean	351	505	447	56	940
	stdev.	695	326	195	12	881
	median	69	514	436	54	597
	min	0.79	1.3	63	26	12
	max	3507	1422	1198	89	5115
2-7 km	mean	68	292	197	25	388
	stdev.	79	244	243	15	413
	median	38	189	133	21	255
	min	5.1	89	49	7.1	59
	max	688	998	2028	71	3341
>7 km	mean	132	282	152	21	416
	stdev.	172	157	191	15	327
	median	41	236	86	23	295
	min	8.3	80	41	3.6	60
	max	557	550	1030	50	1123
Central						
0-2 km	mean	395	1225	1323	69	2422
	stdev.	437	1014	1293	33	2248
	median	276	888	833	58	1723
	min	25	2.4	222	25	222
	max	3111	4264	7412	214	13487
2-7 km	mean	48	194	202	20	297
	stdev.	44	69	110	5.1	150
	median	33	175	169	19	276
	min	1.1	118	106	9.1	65
	max	205	364	938	30	938
Coastal						
0-2 km	mean	34	207	439	11	541
	stdev.	89	336	365	20	525
	median	6.5	19	322	25	386
	min	0.52	1.3	128	10	56
	max	581	1065	2120	104	3267
2-7 km	mean	40	142	439	17	431
	stdev.	42	126	365	7.9	260
	median	29	115	326	13	475
	min	6.3	15	135	10	24
	max	247	412	876	33	1096

Table 1. Continued.

SE Asia						
0-2 km	mean	81	46	139	3.7	218
	stdev.	187	51	217	4.3	273
	median	9.4	16	65	8.1	91
	min	9.0	2.7	12	3.2	6.4
	max	836	237	884	19	1158
2.7 km	mean	81	157	338	10	384
	stdev.	187	190	233	11	330
	median	9.4	80	240	5.4	306
	min	1.1	8.4	100	3.1	5.0
	max	836	660	1352	45	1439
7-12.5 km	mean	39	81	102	3.2	174
	stdev.	32	58	78	4.2	108
	median	38	91	83	6.2	162
	min	1.3	6.2	3.0	2.3	5.8
	max	139	238	320	20	495
WSW						
2-7 km	mean	70	172	137	8.8	240
	stdev.	46	62	47	2.8	118
	median	45	172	130	8.3	211
	min	7.8	78	81	5.0	81
	max	154	311	306	14	569
7-12.5 km	mean	112	258	138	8.5	309
	stdev.	66	182	170	5.1	249
	median	106	186	106	7.1	247
	min	12	30	25	1.8	3.5
	max	354	699	1987	23	2257

***** Sum of the individual species (see text).

Table 2. PEM-WEST B Nitrogen Budget Summary Statistics

Source Region		NO	PAN	HNO_3	Sum Alkyl ONO_2	NO_y*
Continental North						
0-2 km	mean	31	559	617	NA	1084
	stdev.	67	434	1263	NA	1587
	median	18	134	229	NA	624
	min	3.1	54	30	NA	123
	max	937	2187	6596	NA	10243
2-7 km	mean	16	289	168	NA	449
	stdev.	18	190	166	NA	305
	median	13	108	126	NA	406
	min	2.6	1.7	37	NA	64
	max	568	885	1115	NA	1923
>7 km	mean	49	177	166	NA	473
	stdev.	68	164	69	NA	208
	median	39	98	146	NA	449
	min	7.4	20	62	NA	153
	max	833	965	389	NA	1033
Continental South						
0-2 km	mean	13	78	615	NA	941
	stdev.	7.8	82	316	NA	1114
	median	6.8	6.4	548	NA	721
	min	4.6	6.4	219	NA	159
	max	40	247	1275	NA	7029
2-7 km	mean	15	35	455	NA	279
	stdev.	7.8	22	344	NA	206
	median	17	13	421	NA	257
	min	4.5	5.4	55	NA	75
	max	30	68	1225	NA	868
>7 km	mean	57	57	124	NA	234
	stdev.	34	28	47	NA	132
	median	56	38	122	NA	243
	min	7.9	8.8	55	NA	68
	max	339	149	279	NA	540

***** As measured with a gold catalytic converter (see text).

Figure Captions

1. Latitudinal distribution of mixing ratios of NO_y and CO over the western Pacific west of 150ºE longitude. Data is shown for three altitude bins of 0-2, 2-7, and >7 km.
2. Relationships between mixing ratios of NO_y and CO or O_3 in three altitude bins of 0-2, 2-7, and >7 km.
3. Latitudinal distribution of individual NOy species in three altitude bins of 0-2, 2-7, and >7 km.
4. Vertical distribution of individual NO_y species over the western Pacific west of 150ºE longitude.
5. Vertical and longitudinal distributions of the C_2H_2/CO ratio over the western Pacific west of 150ºE longitude.
6. Geographic representation of the five principal source regions on the Asian continent determined from analysis of air parcel isentropic backward trajectories.
7. NO_y budget comparison for the five Asian source regions as a function of altitude (0-2, 2-7, and >7 km). Median values were used for to construct these budgets.
8. Relationships between NO_y and C_2H_2 for each of the five Asian source regions. C_2H_2 is a unique indicator of combustion emissions.
9. Relationship between NO_x and H_2O vapor (red) and dew point temperature (blue) in upper tropospheric air parcels originating over the WSW source region.
10. Relationships between NO_y and C_2Cl_4 for each of the five Asian source regions. C_2Cl_4 is an indicator of urban/industrial emissions.
11. Relationships between NO_y and CH_3Cl for each of the five Asian source regions. CH_3Cl is an indicator of biomass burning emissions.

12. Chemical relationships and breakdown of individual NO_y species in the Shanghai mega-city plume.

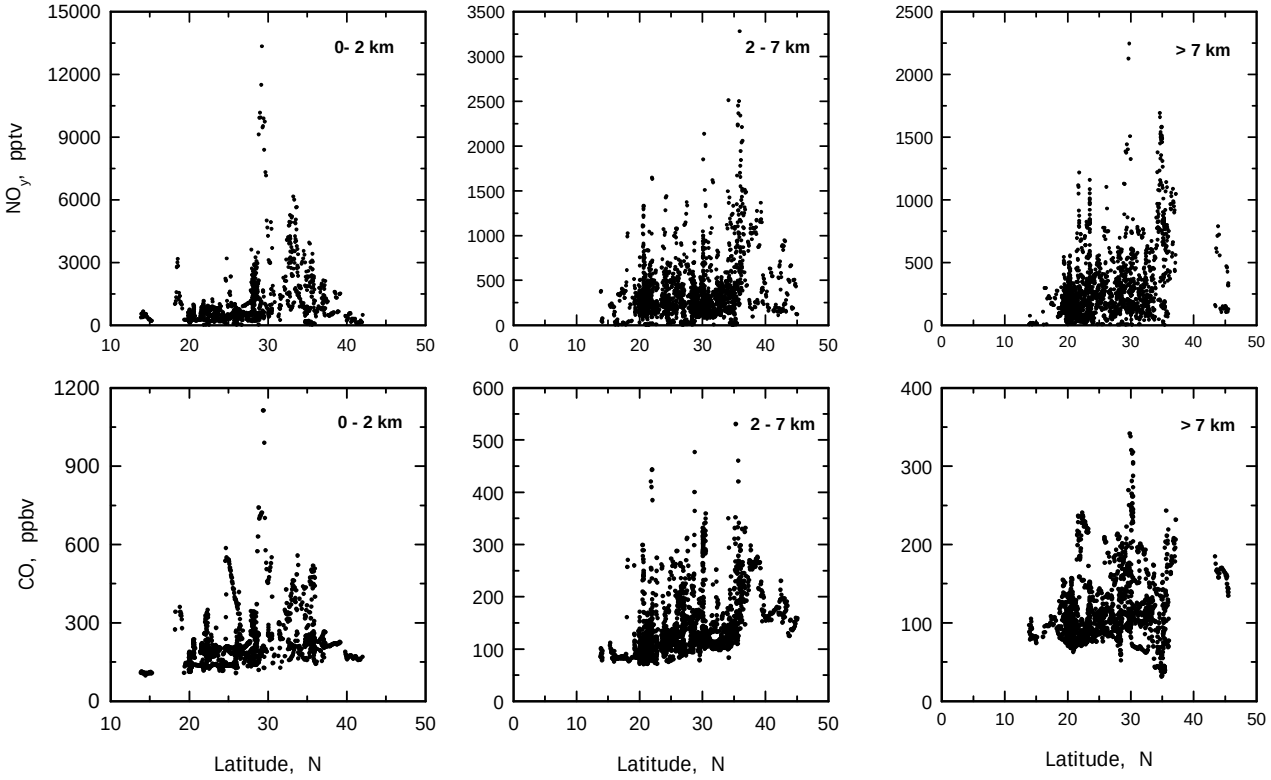
0- 2 km
2 - 7 km
> 7 km
0 - 2 km
2 - 7 km
> 7 km
NOy, pptv
CO, ppbv
Latitude, N
Latitude, N
Latitude, N

Figure 1.

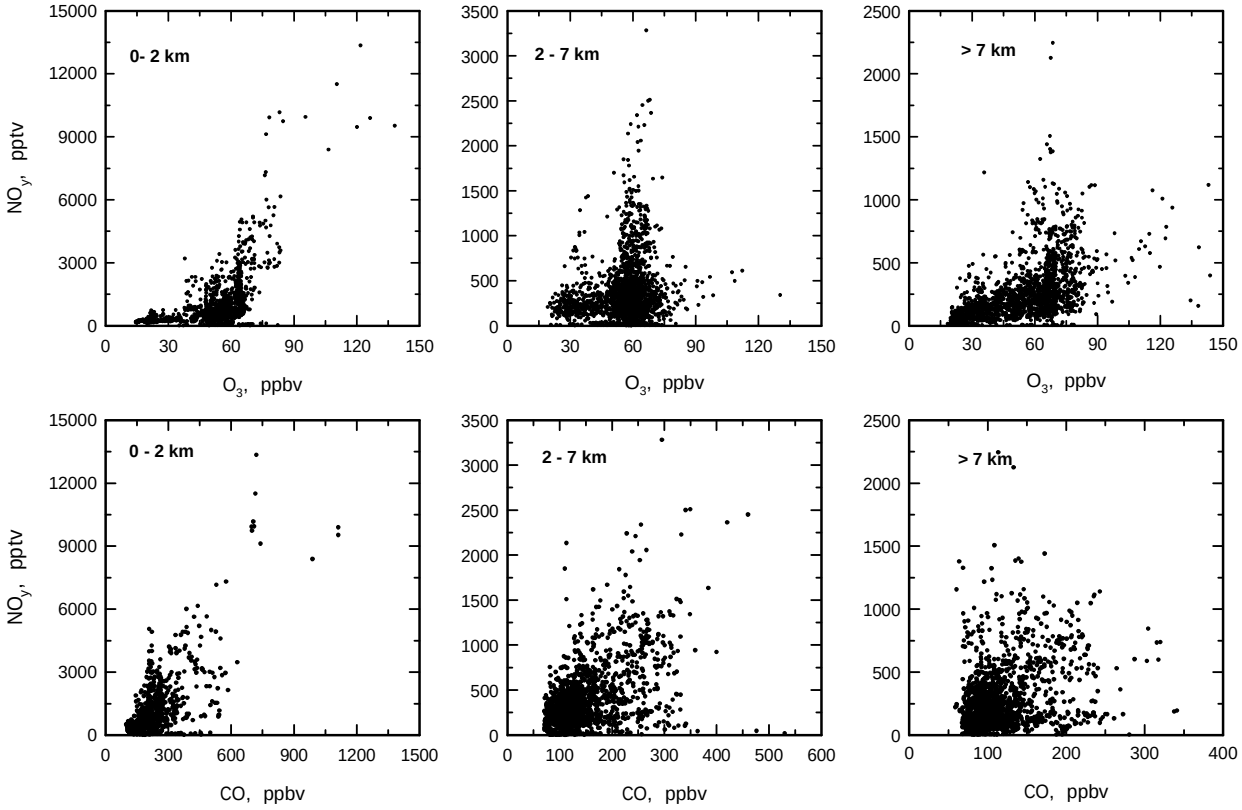

Figure 2.

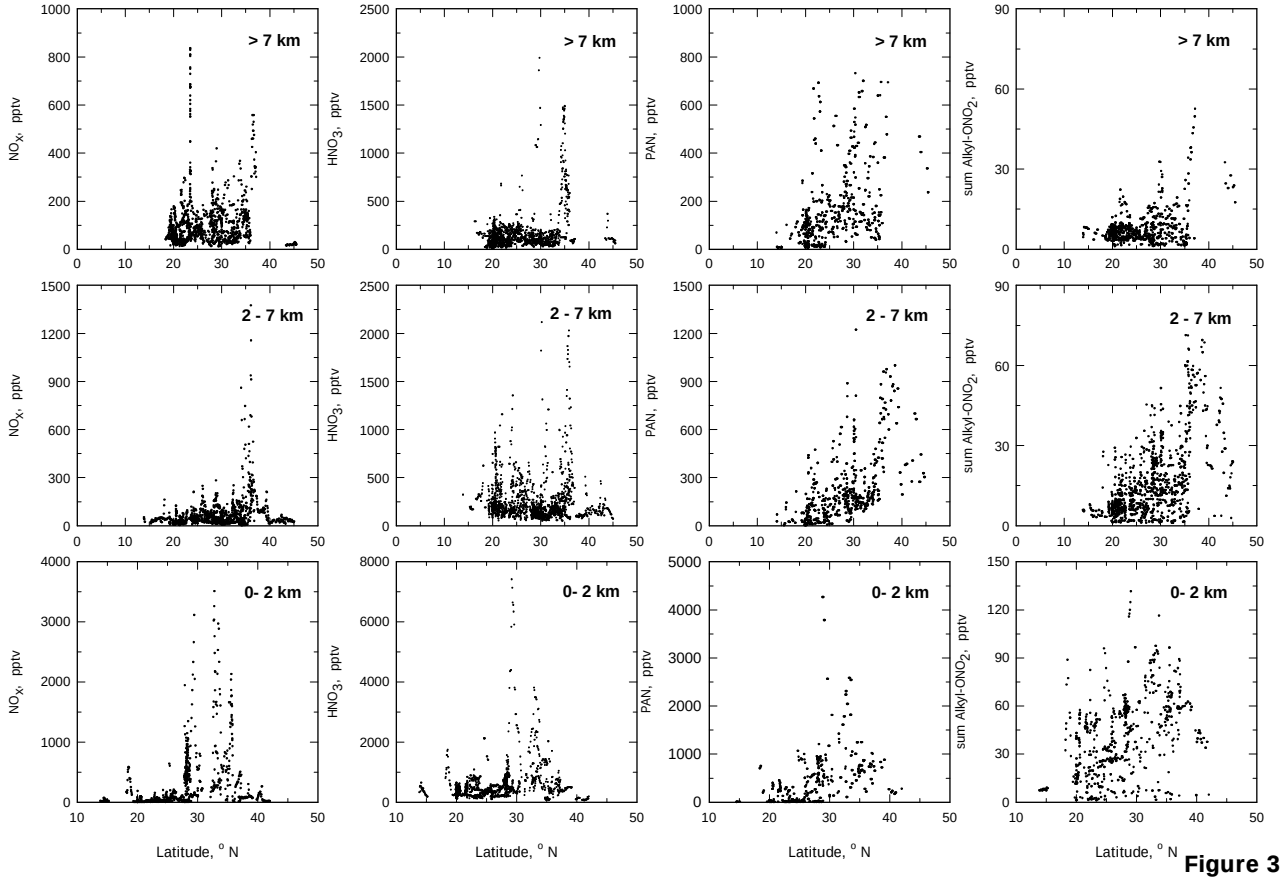
> 7 km
2 - 7 km
0- 2 km
NOX, pptv
HNO3, pptv
PAN, pptv
sum Alkyl-ONO2, pptv
Latitude, ° N

Figure 3.

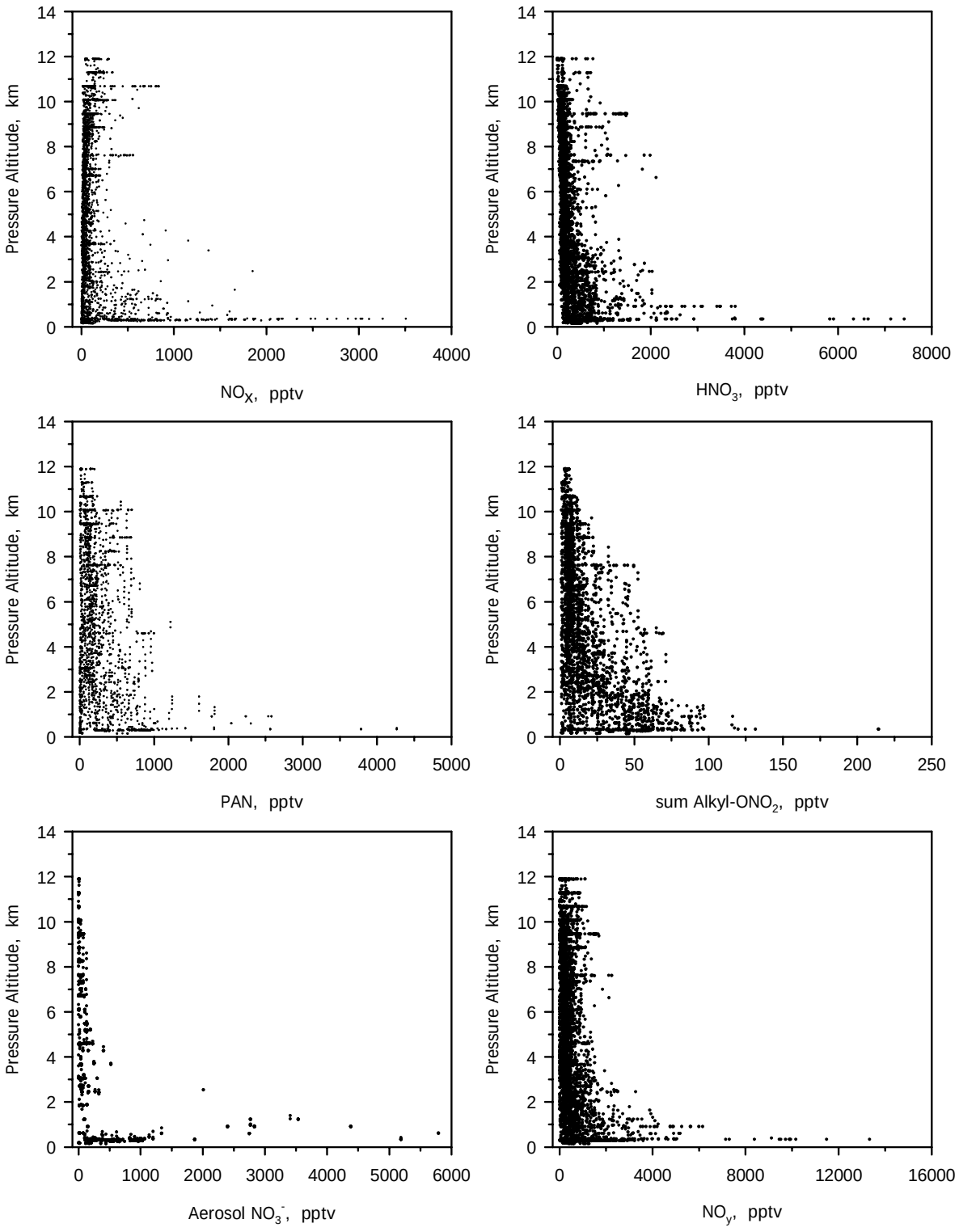
Pressure Altitude, km
NO_X, pptv
HNO_3, pptv
PAN, pptv
sum Alkyl-ONO_2, pptv
Aerosol NO_3^-, pptv
NO_y, pptv

Figure 4.

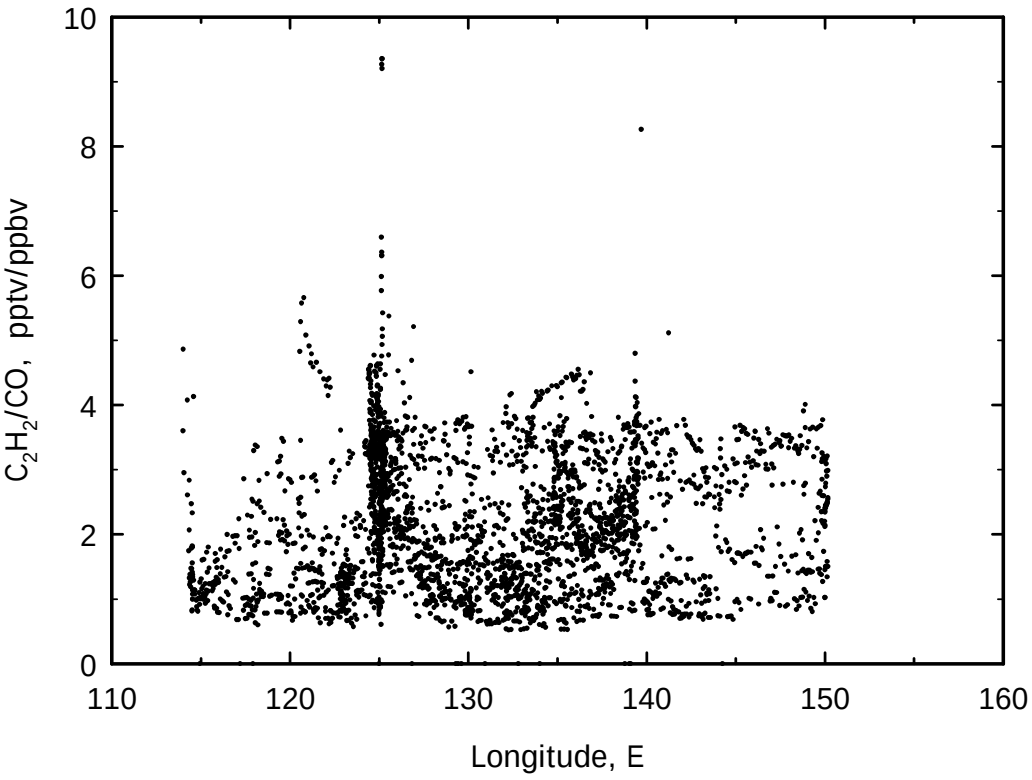
10
8
6
4
2
0
110
120
130
140
150
160
C_2H_2/CO, pptv/ppbv
Longitude, E

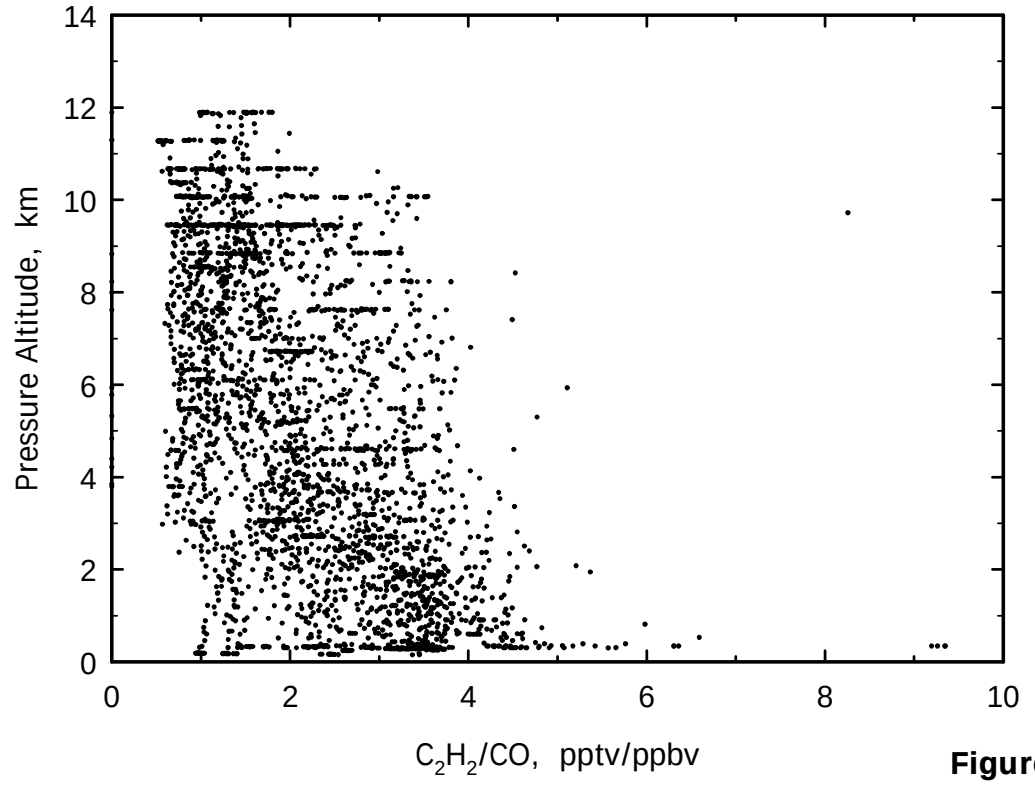
14
12
10
8
6
4
2
0
0
2
4
6
8
10
Pressure Altitude, km
C_2H_2/CO, pptv/ppbv

Figure 5.

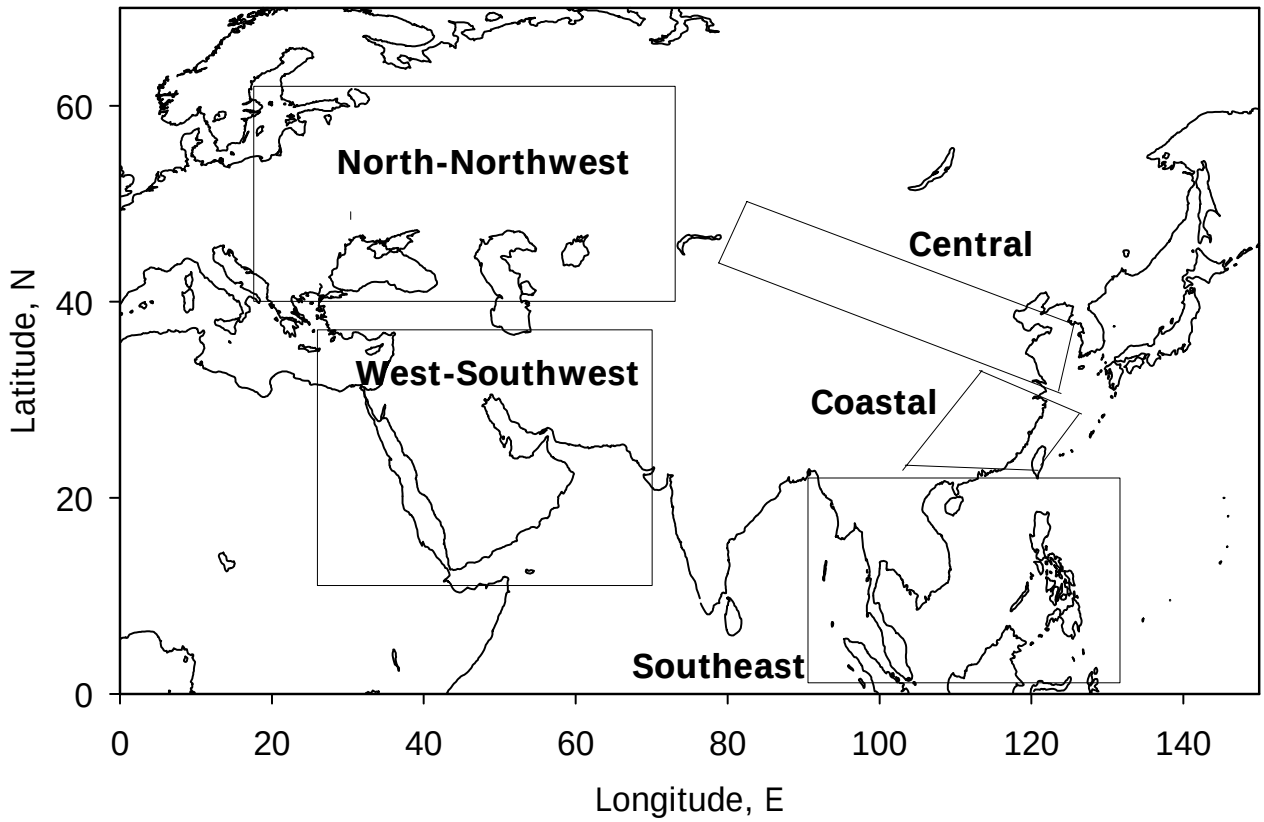
North-Northwest
Central
West-Southwest
Coastal
Southeast
Latitude, N
Longitude, E
0
20
40
60
80
100
120
140
0
20
40
60

Figure 6.

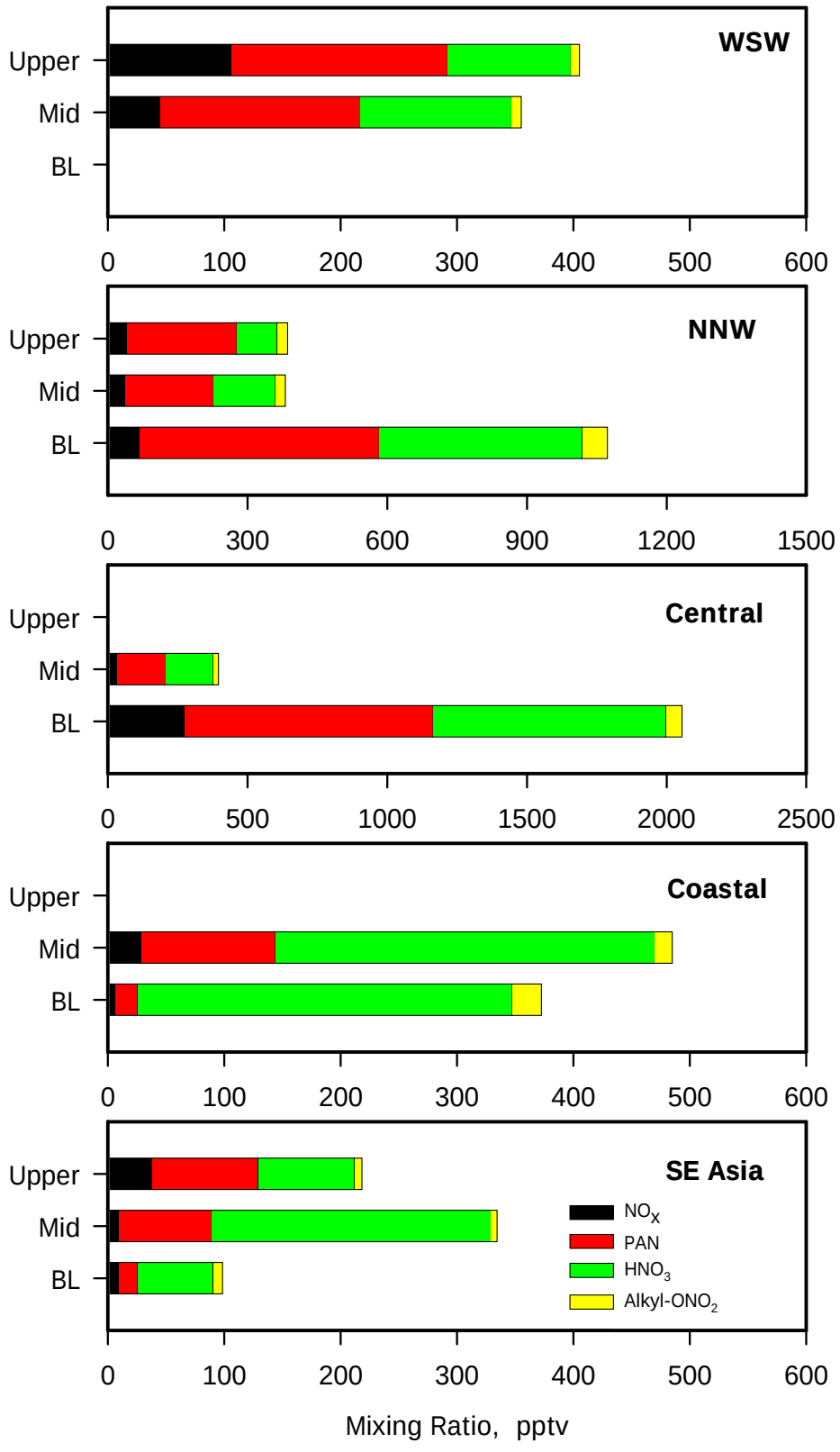
WSW
Upper
Mid
BL
0
100
200
300
400
500
600
NNW
Upper
Mid
BL
0
300
600
900
1200
1500
Central
Upper
Mid
BL
0
500
1000
1500
2000
2500
Coastal
Upper
Mid
BL
0
100
200
300
400
500
600
SE Asia
Upper
Mid
BL
0
100
200
300
400
500
600
NOX
PAN
HNO3
Alkyl-ONO2
Mixing Ratio, pptv

Figure 7.

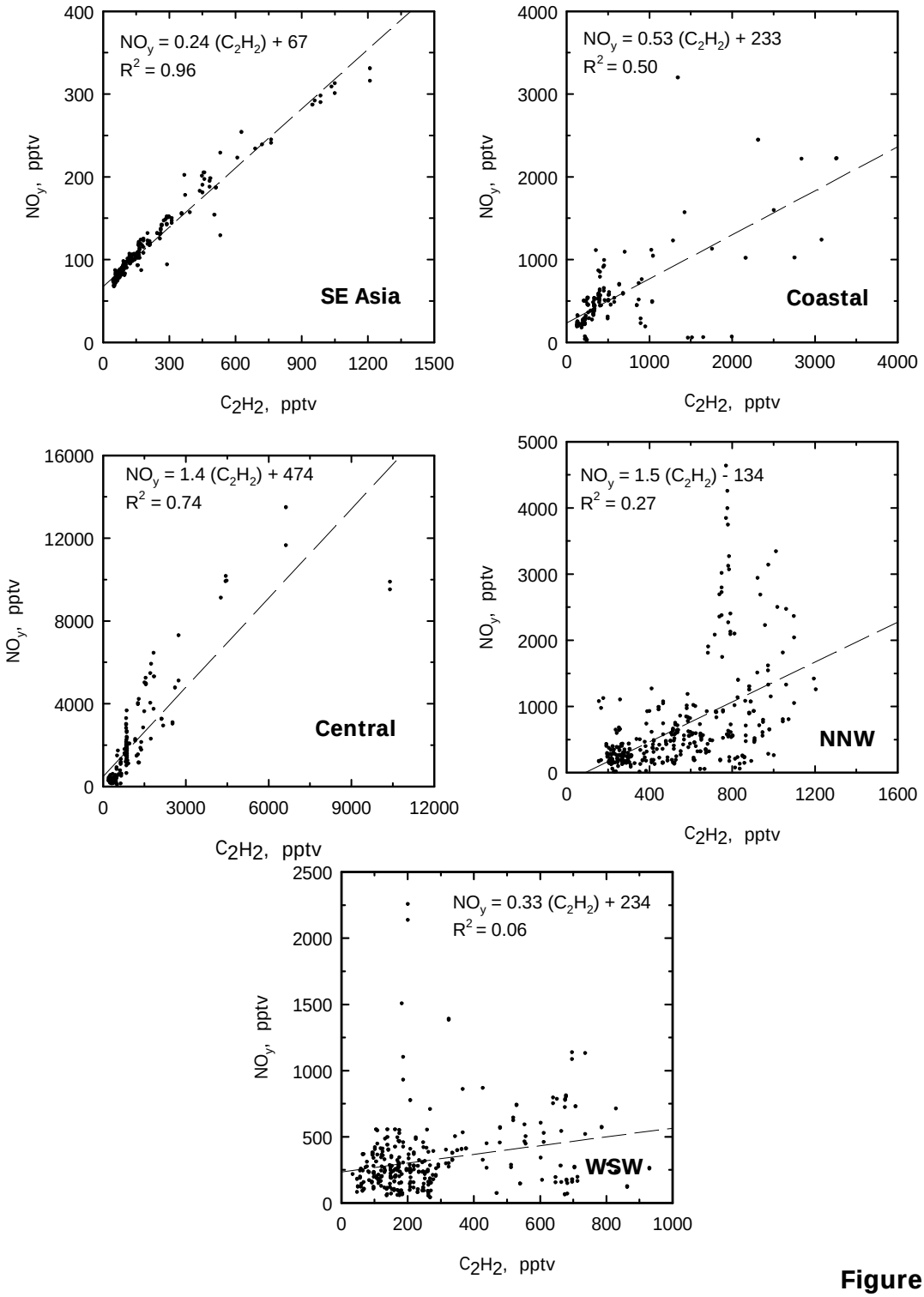
NOy = 0.24 (C2H2) + 67
R2 = 0.96
SE Asia
NOy, pptv
C2H2, pptv
NOy = 0.53 (C2H2) + 233
R2 = 0.50
Coastal
NOy = 1.4 (C2H2) + 474
R2 = 0.74
Central
NOy = 1.5 (C2H2) - 134
R2 = 0.27
NNW
NOy = 0.33 (C2H2) + 234
R2 = 0.06
WSW

Figure 8.

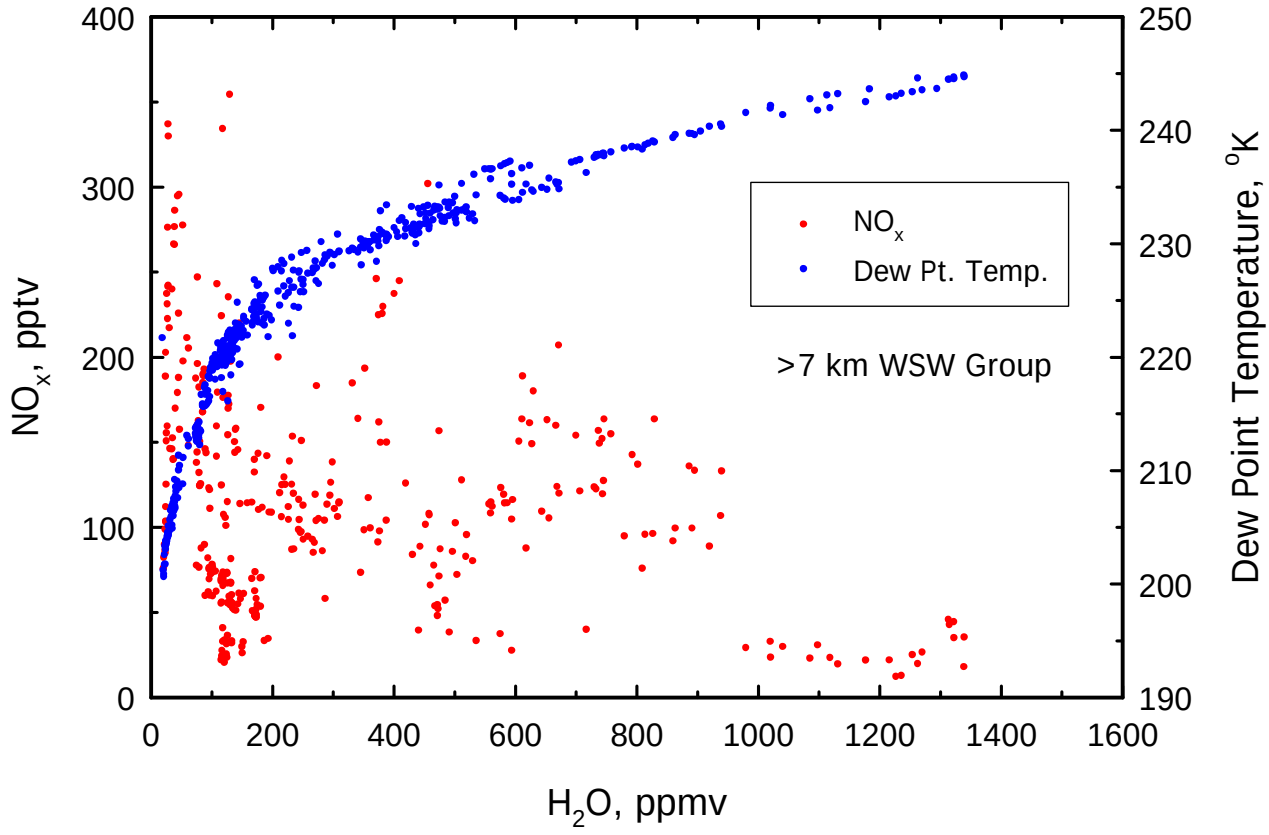
400
300
200
100
0
250
240
230
220
210
200
190
0
200
400
600
800
1000
1200
1400
1600
NOx, pptv
H2O, ppmv
Dew Point Temperature, °K
NOx
Dew Pt. Temp.
>7 km WSW Group

Figure 9.

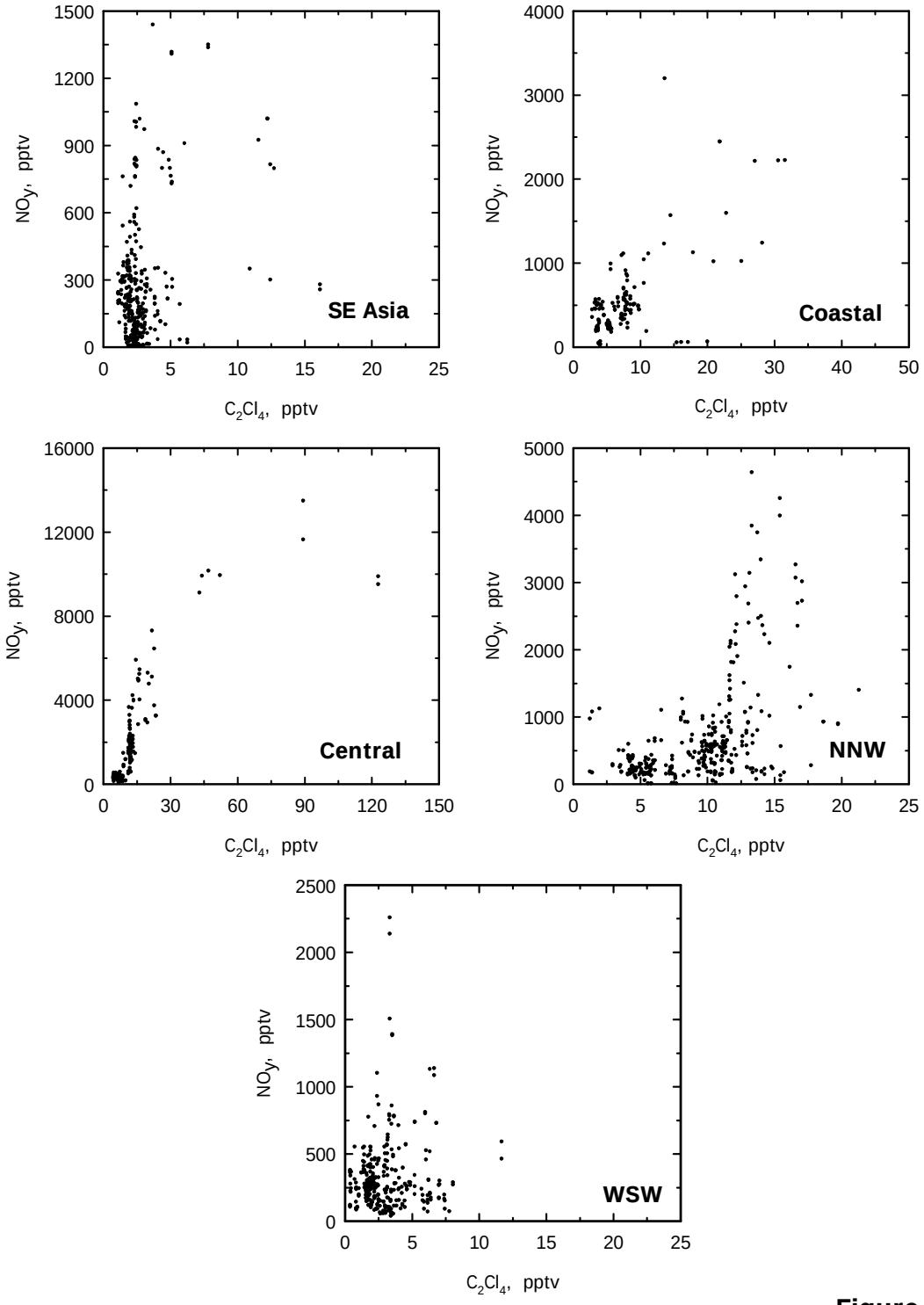

Figure 10.

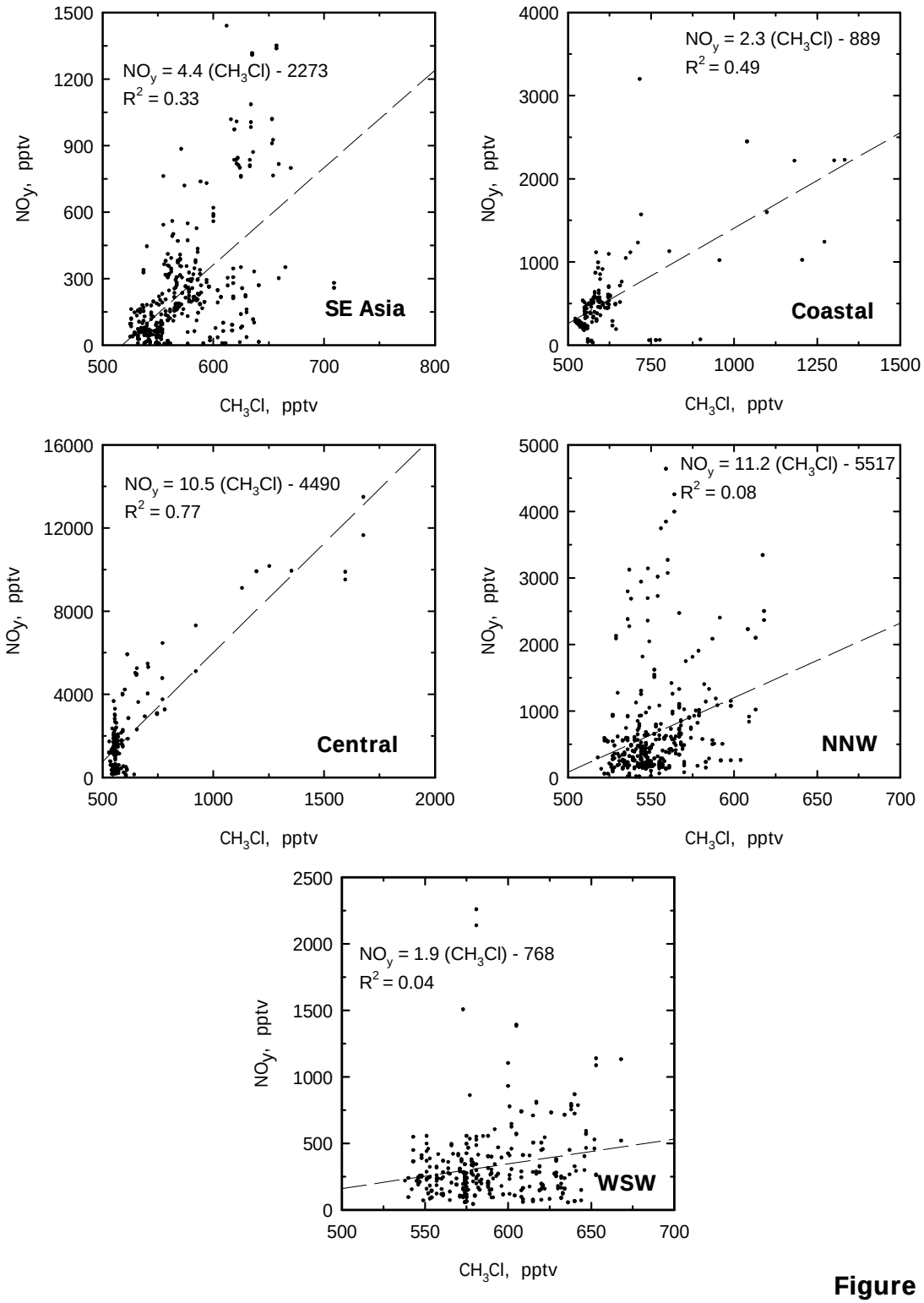
NOy = 4.4 (CH3Cl) - 2273
R2 = 0.33
SE Asia
NOy, pptv
CH3Cl, pptv
NOy = 2.3 (CH3Cl) - 889
R2 = 0.49
Coastal
NOy = 10.5 (CH3Cl) - 4490
R2 = 0.77
Central
NOy = 11.2 (CH3Cl) - 5517
R2 = 0.08
NNW
NOy = 1.9 (CH3Cl) - 768
R2 = 0.04
WSW

Figure 11.

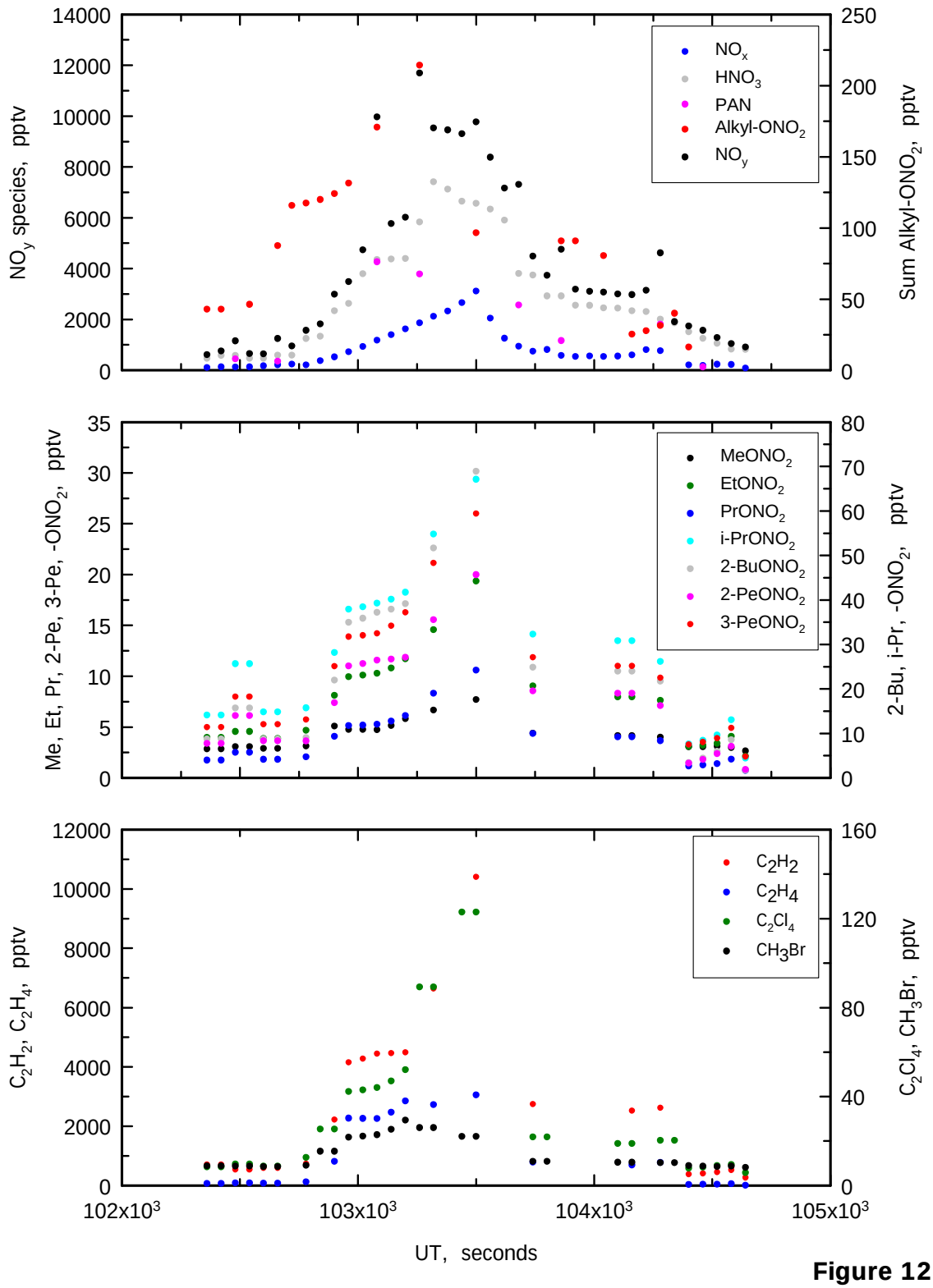
NO$_y$ species, pptv
Sum Alkyl-ONO$_2$, pptv
NO$_x$
HNO$_3$
PAN
Alkyl-ONO$_2$
NO$_y$
Me, Et, Pr, 2-Pe, 3-Pe, -ONO$_2$, pptv
2-Bu, i-Pr, -ONO$_2$, pptv
MeONO$_2$
EtONO$_2$
PrONO$_2$
i-PrONO$_2$
2-BuONO$_2$
2-PeONO$_2$
3-PeONO$_2$
C$_2$H$_2$, C$_2$H$_4$, pptv
C$_2$Cl$_4$, CH$_3$Br, pptv
C$_2$H$_2$
C$_2$H$_4$
C$_2$Cl$_4$
CH$_3$Br
102x10^3
103x10^3
104x10^3
105x10^3
UT, seconds

Figure 12.